

## Bi-axial dielectric anisotropy of crystalline materials and its characterization by resonance microwave methods

P. I. Dankov\*, M. T. Iliev, V. P. Levcheva

Sofia University "St. Kliment Ohridski", Faculty of Physics, 5 J. Bourchier Blvd., 1164 Sofia, Bulgaria

Received October 15, 2018; Accepted November 30, 2018

In this paper, the dielectric parameters (permittivity and dielectric loss tangent) of different single and poly-crystalline or crystalline-like samples have been characterized in the microwave range (especially in the C and X bands; 4–12 GHz). A proven specific property of many crystalline materials is their dielectric anisotropy – different dielectric parameters along different directions and/or crystallographic axes. We consider the anisotropy as a very informative parameter for the sample structure, composition, inclusions, used technology and conditions for the crystal growth or layer deposition. The authorship two-resonator method or some its variants have been used for characterization of the crystalline samples. A lot of results has been presented for the anisotropy of different materials selected as typical examples (crystals, ceramics, glasses, semi-conductor wafers, unknown composites, carbon-content samples: graphite, Graphene, etc.), with different shapes (disks, prisms, cylinders, multilayer composites, thin films, etc.) and different orientation (sample axes orientated along crystallographic axes or in arbitrary directions). Depending on the samples' kind, the observed anisotropy falls in the intervals from 0.35 up to 3.50. The presented data set for the dielectric properties show good correlation with the sample structure and used technology and allow a reliable microwave characterization of the samples, which can add new useful information to the results, obtained by other standard experimental methods applicable for crystals.

**Keywords:** crystals, dielectric anisotropy, microwave methods, permittivity.

### INTRODUCTION

The determination of the dielectric properties of single and poly-crystalline materials (dielectric constant or permittivity  $\epsilon$ , and dielectric loss tangent  $\tan\delta$ ) [1] is a classical problem in the microwave frequency range. There exist different methods for characterization of the dielectric properties of crystals; the most accurate are the resonance ones [2]. However, an additional circumstance for these materials is the presence of relatively strong bi-axial anisotropy in many cases, which usually is not taken into account – different dielectric parameters along the different axes, e.g.  $\epsilon_{xx} \neq \epsilon_{yy} \neq \epsilon_{zz}$  and  $\tan\delta_{\epsilon_{xx}} \neq \tan\delta_{\epsilon_{yy}} \neq \tan\delta_{\epsilon_{zz}}$ . The anisotropy can be calculated as ratios  $A_{\epsilon_{x,y}} = \epsilon_{xx}/\epsilon_{zz}$  or  $\epsilon_{yy}/\epsilon_{zz}$  and  $A_{\tan\delta_{\epsilon_{x,y}}} = \tan\delta_{\epsilon_{xx}}/\tan\delta_{\epsilon_{zz}}$  or  $\tan\delta_{\epsilon_{yy}}/\tan\delta_{\epsilon_{zz}}$ . In principle, these materials are homogeneous, but the tightly packed and orientated building blocks of the crystals act as interacting electrical dipoles, which orientation in the

high-frequency electric fields causes the observed anisotropy. The possible inclusions in the crystal lattice also influence the anisotropy. Due to these and additional reasons the crystalline dielectric anisotropy  $A_{\epsilon_{x,y}}$  and  $A_{\tan\delta_{\epsilon_{x,y}}}$  could be very informative parameters for the sample composition, inclusions, used technology and conditions for the samples' formation. However, the possible anisotropy makes the characterization of the crystalline dielectric parameters more difficult and the most of the known measurement methods cannot give any information for this parameter. Fortunately, we have developed a set of authorship resonance methods, which allow accurate determination of the dielectric anisotropy of different materials, including crystalline samples. One of the most efficient is the two-resonator method [3, 4] and some its modifications [5, 6].

In this paper, we continue to develop reliable measurement methods especially for determination of the dielectric anisotropy of crystalline materials and to show how this parameter could be bound with other sample parameters and formation conditions. We have presented several typical situations for characterization of different crystalline and crys-

\* To whom all correspondence should be sent:  
E-mail: dankov@phys.uni-sofia.bg

talline-like samples from different types: ceramics, glasses, mono- and poly-crystals, semiconductors, ferrites, metamaterials; also samples with different shapes: cylinders, disks, prisms, planar substrates, thin layers, multi-layer composites, etc. The extraction of the dielectric parameters  $\epsilon_{xx, yy, zz}$  and  $\tan\delta_{xx, yy, zz}$  has been realized by simulations of synthesized 3-D models of the resonance structures, measured with and without samples, through 3-D electromagnetic simulator ANSYS®HFSS in eigen-mode option [7] and the corresponding anisotropy parameters  $A_{\epsilon_{x,y}}$  and  $A_{\tan\delta_{x,y}}$  have been calculated, compared and discussed.

### MEASUREMENT METHOD

The complex permittivity  $\epsilon_c$  of the materials in the microwave region varies between the dc permittivity  $\epsilon_{dc}$  at very low frequencies up to optical value  $\epsilon_{\infty}$  at very high frequencies according to the known Cole-Cole model [8]. Exactly due to this reason the “microwave” complex permittivity  $\epsilon_{MW}$  of the crystals could be enough informative for the relaxation mechanism understanding, specific crystal structure, used inclusions and other properties of these materials. However, due to the difficulties for the samples’ preparation, their specific forms, small sizes, etc., the most of the crystalline and crystalline-like materials could not be measured by the popular free-space and transmission-line methods, based on relatively big samples. Only the rectangular wave-guide method is able to determine the crystal permittivity and even crystals’ anisotropy [2]. The resonance methods, which are more accurate in comparison to the waveguide methods, also meet some difficulties, mainly due to the large values of the permittivity and needs for reliable mode identifications in the resonator spectrum with sample.

In [3–5] we describe in details the so-called two-resonator method, developed especially for determination of the dielectric anisotropy in flat planar single- and multi-layer samples. The method is based on measurements of the resonance parameters (resonance frequencies and unloaded quality (Q-) factors) of two cylinder resonators with different height, which support modes  $TE_{011}$  and  $TM_{010}$  with mutually perpendicular electric fields – see the schematic illustrations in Fig. 1. The sample under test can fill the entire cross section of the resonators or may have smaller sizes. In the first case, when the sample is a disk with diameter coinciding with the resonator diameter, the dielectric parameters of the materials could be extracted by the analytical model, introduced in [3, 4]. The extraction of the dielectric parameters in the second case, when the sample has arbitrary, but regular shape and sizes, is based on 3-D simulations of well-constructed 3-D model of the measurement resonator with sample following the procedure, described in [5]. The measurement accuracy in the both cases has been ensured by introducing of equivalent dimensions and conductivity of the metallic walls after measurement of the empty resonator, which takes into account their deviation from the ideal shape and the wall roughness. Based on these simple measurement principles, we managed to determine the dielectric parameters and especially to estimate with satisfied accuracy the dielectric anisotropy of many samples, including microwave hard and artificial soft ceramics [5].

The described above two-resonator method is convenient for dielectric anisotropy characterization of thin substrates with equal diameter (but for different frequencies) or with different diameters at close frequencies; samples with relatively small sizes are also applicable. Due to the cylindrical symmetry, the method gives the so-called uni-axial anisotropy – only the pair of the parallel and perpendicular die-

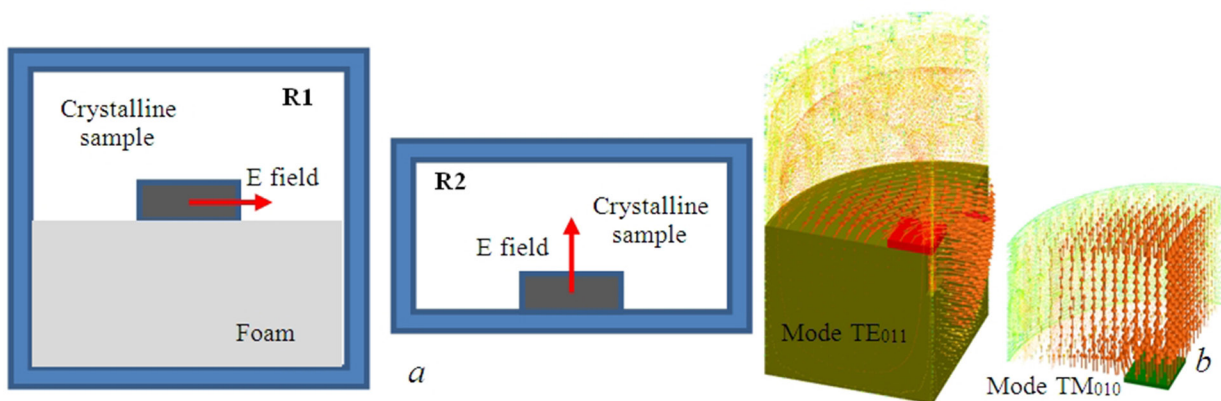


**Fig. 1.** Two-resonator method (resonators R1, R2) (a) and electric (E-) field distribution (b).

lectric parameters, i.e.  $\epsilon_{par} = \epsilon_{xx} = \epsilon_{yy}$ ;  $\tan\delta_{epar} = \tan\delta_{exx} \neq \tan\delta_{eyy}$  and  $\epsilon_{perp} = \epsilon_{zz}$ ;  $\tan\delta_{eperp} = \tan\delta_{ezz}$ . For bulk samples with regular shapes (prisms or cylinders) and sizes smaller than the resonator diameter and height, more reliable is the measurement method, based on application of a single resonator (either R1 with TE<sub>011</sub> mode TM<sub>010</sub> or R2 with TM<sub>010</sub> mode), when each sample has been placed in three different orientations according to the resonator axis – see illustrations in Fig. 2, 3. In the case of prism samples, the actual bi-axial anisotropy could be determined: full set of parameters:  $\epsilon_{xx,yy,zz}$  and  $\tan\delta_{exx,yy,zz}$ .

The symmetry of the presented measurement structures with and without sample allows to split twice the corresponding 3-D models and to make the simulations more time efficient and accurate. However, specific symmetrical boundary conditions should be applied in this case at the splitted surfaces: E-field symmetry – for parallel E fields along the surface and H-field symmetry – for perpendicular E field [7] (Fig. 3).

The proven measurement accuracy for the two-resonator method is  $\pm 5\%$  for the dielectric constant anisotropy and up to  $\pm 15\%$  for the dielectric loss tangent anisotropy [3] for relatively thin disk samples (thickness  $\sim 0.5\text{--}1.5$  mm and dielectric constant less than 10). The accuracy decreases for thicker cylinders and prisms, very thin layers and for high-permittivity materials due to different reasons: screening effect of the resonator walls; appearance of parallel E-field components in TM-mode resonator and v.v., sample preparation; accuracy for determination of the actual sample dimensions, etc.

## RESULTS AND DISCUSSION

In this section of the paper we present and discuss the results for the dielectric parameters and dielectric anisotropy of several typical crystalline and crystalline-like materials by the described resonance methods in the C and X bands (4–12 GHz). In

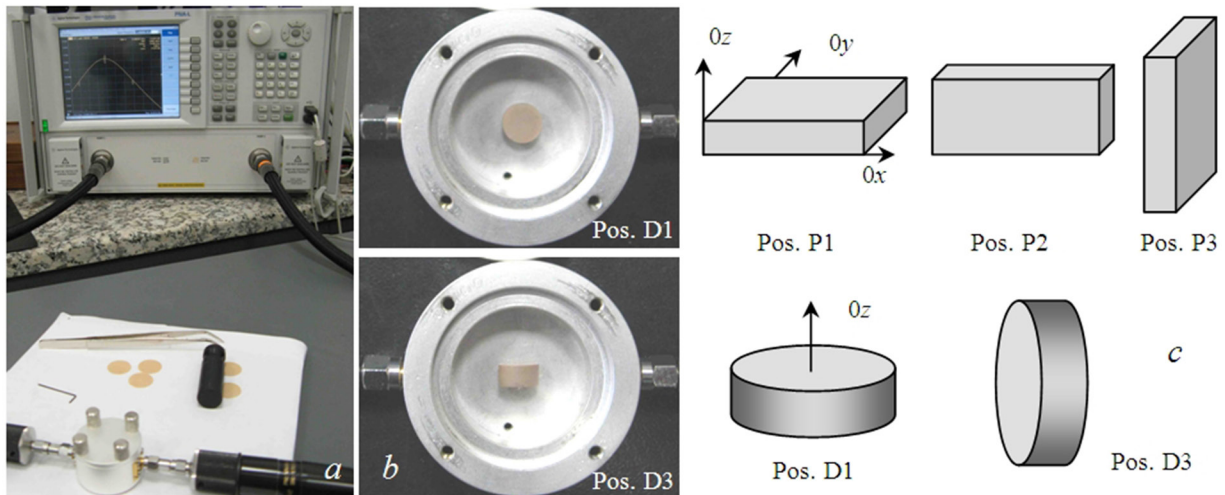


**Fig. 2.** Measurement setup (a); resonator R2 with disk samples in two positions (b); possible positions inside the resonator of prism and disk (cylinder) samples (c).

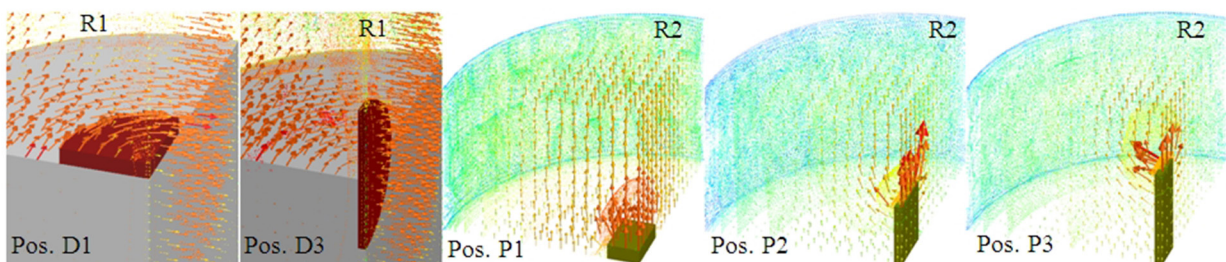


**Fig. 3.** Illustration of the E-field vector distribution in the measurement resonators R1 and R2 with disk and prisms samples in different positions as in Fig. 2.



fact, the two-resonator method and its variants have been applied for characterization of huge amount of different samples in the last 15 years: microwave substrates [5], multi-layer antenna radomes [3], ceramics and ferrites [4, 9, 10], thin layers [11], foams, absorbers [12] and recently textile fabrics [13], fresh plant tissues [14], 3-D printed materials [15] and even metamaterials [16]. Therefore, we selected here several very typical cases with some older results and many new data for application of the authorship two-resonator method for this class of materials, which could be considered as lattices with ordered building blocks, i.e. crystals, crystal-line-like materials and some metamaterials.

Let's start with the ceramics and high-permittivity (high-K) substrates with mic-rowave applications. Actually, the microwave engineers know the dielectric anisotropy phenomena mainly from some of the first applications of the Alumina ( $Al_2O_3$ ) ceramics and Sapphire ( $\alpha-Al_2O_3$ ) substrates for micro-strip lines with very low losses (e.g. see [17, 18]). Another high quality materials as substitute of the Alumina is the Polycore ( $Al_2O_3 + 0.3\% MgO$ ). The glass ceramic material Sitall was a solution for good microwave substrate with slightly bigger losses, but with extremely low temperature coefficient of expanding. These materials were the basics for the

starting of the first planar hybrid microwave integrated schemes (MIC's) since more than 40 years. These materials are low-loss and relatively high-K, suitable for compact MIC's, but the relatively big difference between the absolute values of the parallel and perpendicular dielectric constants was a serious design problem; rows 1, 2 in Table 1. The measured anisotropy  $A_e$  of these first microwave ceramics falls in relatively narrow interval 0.93–1.15; however, due to their high-K properties the absolute difference between the permittivity values in the both directions is relatively big; definitely, this was a serious design problem in these early stages of the hybrid MICs [7]. Another, more isotropic alternative was the fused Quartz substrate (the anisotropy is several times smaller – see the corresponding values in Table 1, row 4), but this substrate was very unacceptable from technological point of view. Then the substrate producers began to offer attractive artificial soft ceramics – plastic substrates with high-K ceramic filling. One of the first soft ceramics were 3M®Epsilam10 and then the popular now materials Rogers® Ro3010, TMM10i and RT Duroid®6010. However, these new artificial ceramics even have bigger anisotropy (see data in rows 5–9 in Table 1). They again consist of ordered non-spherical grains (ceramic inclusions); if

**Table 1.** Dielectric parameters and uni-axial anisotropy of some ceramic substrates, measured by the two-resonator method [3–5]

No	Material Reference values	Shape	$D, h, mm$	Freq. bands	parallel: $\epsilon_{par}; \tan\delta_{epar}$	perpendicular: $\epsilon_{perp}; \tan\delta_{eperp}$	anisotropy: $A_e; A_{\tan\delta_e}$
1	Corsa® Alumina ( $Al_2O_3$ ) 9.8-10.7	disk	$\phi 30; 0.6$	C, X	9.65/0.0003	10.35/0.0004	0.93/0.75
2	Polycore ( $Al_2O_3 + 0.3\%$ MgO)	disk	$\phi 30; 0.5$	C, X	10.035/0.0002	9.21/ 0.0003	1.09/0.67
3	Sitall (glass ceramic)	disk	$\phi 30; 0.635$	C, X	8.19/0.0042	7.16/ 0.0038	1.14/1.11
4	Fused quartz	disk	$\phi 30; 0.8$	C, X	4.38/~0.0001	4.26/~0.0001	1.03/~1
5	3M® Epsilam 10 9.8/0.0020	disk	$\phi 30; 0.635$	C, X	11.64/0.0022	9.25/0.0045	1.26/0.49
6	Rogers® TMM10i 9.80/0.0020	disk	$\phi 30; 0.635$	C, X	11.04/0.0019	10.35/0.0035	1.07/0.54
7	Rogers® Ro3010 10.20/0.0035	disk	$\phi 30, 18;$ $0.635$	C, X, Ku	11.74/0.0025	10.13/0.0038	1.16/0.66
8	Rogers® Ro3010 10.20/0.0035	disk	$\phi 30, 18;$ $0.25$	X, Ku	11.76/0.0024	9.26/0.0041	1.27/0.59
9	RT Duroid ® 6010 10.2/0.0023	disk	$\phi 30, 18;$ $0.25$	X, Ku	10.71	10.252	1.045
10	ACX® LTCC 7.5/0.003	disk	$\phi 30, 18;$ $0.2; 2.0$	X, Ku	7.60/0.007	6.68/0.0075	1.13/0.93
11	ACX® LTCC 7.5/0.003	disk	$\phi 10; 0.2$	Ka	7.90/0.008	6.70/0.0085	1.18/0.94
12	YIG Garnet 14.8; Ms 1.7 kA/cm	disk	$\phi 30; 1.0$	C, X	15.83/0.00020	13.11/0.00027	1.21/0.74

the electric field is orientated along the bigger axis of these ellipses, the resultant dielectric constant increases (the parallel value  $\epsilon_{par}$  in these cases). In fact, the producers introduced also low-permittivity reinforced substrates with bigger success; they have fiber-glass fabrics with ceramic or other filling and the resultant materials are also anisotropic (see data in Table 2). Now the origin of the anisotropy is another – the ordered reinforcing fibers increase the dielectric constant in parallel directions of the planar substrates and the dielectric constants are  $\epsilon_{par} > \epsilon_{perp}$ . In 2002 we were the first researchers [19], which indicated the problem of the dielectric anisotropy in the modern reinforced substrates and introduced the two-resonator method [5], but only after 2009 the bigger substrate producers became to share information for this parameter. Now a new class of microwave ceramics is applicable in the monolithic MIC's and in the devices for millimeter wavelength range – LTCC (low-temperature co-fired ceramics). The LTCC samples are made from many stacked single ceramic layers (each with thickness less than 0.1 mm); this is again a new source of anisotropy, even slightly smaller – see data in rows 10–11 of

Table 1. The LTCC ceramics are nowadays a good substitute of the standard Alumina ceramics, but at higher prices.

Among the ceramic-like materials with microwave applications we can add the microwave ferrites with different composition. They have properties like ceramics (high permittivity; low losses – see Table 1, row 12), but have magnetic properties: saturation magnetization  $M_s$  and relative permeability  $\mu \neq 1$ . Due to this fact, the ferrites are more difficult for characterization of the dielectric parameters (we have special procedure by the two-resonator method, developed for ferrites and ferrite absorber films [10–12]).

The last example for a reliable application of the authorship two-resonator method is connected with characterization of very thin metamaterials (controllable growth metal nanowire inclusions with diameter 30 nm and length 4–6 nm on a thin porous dielectric matrix; the samples have been prepared in the Microelectronic department of the Technical University, Sofia – see Table 3). The samples are really very thin: ~12 nm; they are supported by a pair of thin plastic Kapton disks, because the single

**Table 2.** Dielectric parameters and uni-axial anisotropy of some reinforced substrates, made by fiber-glass fabrics with ceramic filling [5]

No	Substrate; (IPC TM 650 2.5.5.5 ref. data)	$D, h, \text{ mm}$	$f, \text{ GHz} /$ $Q \text{ factor}$	parallel: $\epsilon_{par}; \tan\delta_{epar}$	$f, \text{ GHz} /$ $Q \text{ factor}$	perpendicular: $\epsilon_{perp}; \tan\delta_{eperp}$	anisotropy: $A_\epsilon; A_{\tan\delta\epsilon}$
1	Rogers® Ro4003 (3.38/0.0027)	$\phi 30; 18 \text{ 0.51}$	12.5050/1780	3.67/0.0037	12.4235 /2834	3.38/0.0028	1.086/ 1.32
2	Arlon® 25N (3.38/0.0025)	$\phi 30; 18 \text{ 0.52}$	12.5254/1492	3.57/0.0041	12.4243 /2671	3.37/0.0033	1.059/ 1.242
3	Isola® 680 (3.38/0.0030)	$\phi 30; 18$ 0.525	12.4820/1280	3.71/0.0049	12.4215 /1767	3.32/0.0042	1.117/ 1.167
4	Taconic® RF-35 (3.50/0.0033)	$\phi 30; 18$ 0.512	12.4552/1176	3.90/0.0049	12.4254 /2729	3.45/0.0038	1.130/ 1.289
5	Neltec® NH9338 (3.38/0.0025)	$\phi 30; 18$ 0.520	12.4062/1171	4.02/0.0051	12.4303 /2849	3.14/0.0025	1.280/ 2.040

**Table 3.** Dielectric parameters and uni-axial anisotropy of some crystalline samples, measured by different pairs of measurement resonators by two-resonator method

No	Sample; sizes, mm	$f, \text{ GHz} /$ $Q \text{ factor}$	parallel: $\epsilon_{par}; \tan\delta_{epar}$	$f, \text{ GHz} /$ $Q \text{ factor}$	perpendicular: $\epsilon_{perp}; \tan\delta_{eperp}$	anisotropy: $A_\epsilon; A_{\tan\delta\epsilon}$
1	Sapphire (single crystal) Prism: 17.7×12.5×5.6	6.5510 / 16655	10.1118 / 0.0000293	5.3658 / 3800	8.425 / 0.000001	1.200 / 29.3
2	Sapphire (single crystal) Prism: 10.3×8.0×5.3	9.1840 / 20750	10.2915 / 0.0000302	6.4057 / 3938	7.820 / 0.000005	1.316 / 6.04
3	Quartz (fused) Prism: 12.8×12.3×9.3	9.4450 / 9700	4.462 / 0.0000685	5.3520 / 3766	4.177 / 0.000021	1.068 / 3.26

**Table 4.** Dielectric parameters and uni-axial anisotropy of very thin metamaterial samples with nano-wire inclusions on isotropic Kapton substrates

No	Sample	Shape	$D, \text{mm}; h, \mu\text{m}$	Freq. bands	parallel: $\epsilon_{par}; \tan\delta_{epar}$	perpendicular: $\epsilon_{perp}; \tan\delta_{eperp}$	anisotropy: $A_\epsilon; A_{\tan\delta\epsilon}$
1	1D (nano-wire length 4 nm)	disk	$\phi 18.1; \sim 12$	Ku K	3.780 / 0.0085 4.030 / 0.0094	1.295 / 0.0033 1.180 / 0.0011	2.92/2.58 3.42/8.55
2	2D (nano-wire length 6 nm)	disk	$\phi 18.1; \sim 12$	Ku K	5.450 / 0.0390 6.880 / 0.0382	2.100 / 0.0100 1.580 / 0.0190	2.59/3.90 4.35/2.01
3	Kapton ( $2 \times 50 \text{ mm}$ )	disk	$\phi 18; 100$	Ku K	3.150 / 0.0225 3.184 / 0.0230	3.100 / 0.0217 3.280 / 0.0180	1.16/1.04 0.97/1.28

meta-layer cannot behave as an independent sample. In this specific case, we first have to determine the parameters of the thin support Kapton sample  $\sim 100 \mu\text{m}$  (isotropic, without sample) (see row 3), and then to extract the dielectric parameters of the meta-layers (rows 1–2). We can indicate the very big anisotropy due to the ordered metal nano-wire inclusions;  $A_\epsilon \sim 2.6\text{--}4.4$ .

The next part of our discussion is devoted to the comments of comparative data, obtained by the single-resonator method for crystalline samples (bulk prisms and cylinders) with different orientations (positions P1, P2 and P3 or positions D1, D2 in Fig. 2, 3). Similar to our method with cylindrical resonators is those, described in [20] for rectangular resonator. First of all, we present in Table 5 (for disk/cylinder samples) and Table 6 (for prism samples) dielectric parameters and anisotropy of similar or the same samples as in the previous measurements. Definitely, we obtain very similar results for the already measured samples by other methods, e.g. for LTCC, fused Quartz, Alumina ceramics, etc. In the same time, there appear some well-observed differences for the other samples. The anisotropy of samples from a given materials implemented as a single-crystal or poly-crystalline sample, is different; the single crystals always show bigger anisotropy – see data for samples from Quartz, Sapphire, etc. For example, fused and single-crystal Quartz samples have equal values for

the perpendicular permittivity,  $\epsilon_{zz} \sim 4.27\text{--}4.32$  (the  $c$ -axis coincides with the resonator axis  $0z$ ), while the values for the parallel permittivity  $\epsilon_{xx}, \epsilon_{yy}$  are different:  $\sim 3.74\text{--}3.84$  in the single crystal along the  $a$ -axes;  $\sim 4.31\text{--}4.32$  in the fused Quartz (see rows 1, 2 in Table 6). Similar isotropic-like behavior we observed in the bulk polycrystalline Alumina (row 5); while some glasses with inclusions don't show isotropic behavior (rows 3, 4), opposite to the expectations for such homogenous materials. In fact, most of the selected samples in Tables 5, 6 show more or less expressed anisotropy: Sapphire, Magnesium Titanate  $\text{MgTiO}_3$ , ferrites, etc. (rows 6–8). Mica, a sheet silicate (phyllo-silicate) mineral, includes several closely related layers having nearly perfect basal cleavage, explained by the hexagonal sheet-like arrangement of its atoms. Due to this property Mica sample shows relatively big dielectric anisotropy  $A_\epsilon \sim 1.60$  (row 9). A detectable relatively strong anisotropy we observe also for the presented semiconductor samples – single silicon crystal (for Si wafers) and semi-isolated GaAs for wafers ( $A_\epsilon \sim 1.32\text{--}1.43$ ; rows 10, 11 in Table 6) (the samples have been given up from the Faculty of Physics in Sofia University “St. Kliment Ohridski”).

A very interesting and informative example with completely new results has been presented in Table 7 – results for the dielectric parameters of several Carbon-content disk samples: spectral pure Graphite, air-filled Graphite, tick pressed Graphene

**Table 5.** Dielectric parameters and uni-axial anisotropy of cylinder and disk samples by single resonator method with different sample orientations (cylinder axis is orientated along  $0z$ )

No	Material	$D, \text{mm}; h, \mu\text{m}$	parallel: $\epsilon_{par}; \tan\delta_{epar}$	perpendicular: $\epsilon_{perp}; \tan\delta_{eperp}$	anisotropy: $A_\epsilon; A_{\tan\delta\epsilon}$
1	ACX® LTCC	$\phi 10.98; 1.96$	7.66 / 0.0069	6.20 / 0.0048	1.24/1.44
2	$\text{MgTiO}_3$	$\phi 4.92; 5.02$	14.61 / 0.00028	15.10 / 0.00018	0.97/1.56
3	Alumina ( $\text{Al}_2\text{O}_3$ )	$\phi 8.74; 8.46$	8.40 / 0.000075	9.22 / 0.00006	0.91/1.25
4	Bulk soft ceramic	$\phi 8.02; 10.02$	9.78 / 0.00080	10.20 / 0.00075	0.96/1.07

**Table 6.** Dielectric parameters and bi-axial anisotropy of prism samples by single resonator method with different sample orientations

No	Material	along Ox: $\epsilon_{xx}; \tan\delta_{\epsilon_{xx}}$	along Oy: $\epsilon_{yy}; \tan\delta_{\epsilon_{yy}}$	along Oz: $\epsilon_{zz}; \tan\delta_{\epsilon_{zz}}$	anisotropy: $A_{\epsilon_{xz}}; A_{\tan\delta_{\epsilon_{xz}}}$	anisotropy: $A_{\epsilon_{yz}}; A_{\tan\delta_{\epsilon_{yz}}}$
1	Quartz (single crystal) Prism: 3.00×9.14×10.82	3.74 / 0.00005	3.84 / 0.00005	4.27 / 0.00010	0.88/0.50	0.90/0.50
2	Quartz (fused) Prism: 1.26×7.18×12.0	4.32 / 0.00012	4.31 / 0.00013	4.325 / 0.00041	0.99/0.29	0.99/0.32
3	Silica glass Prism: 3.00×9.14×10.82	5.15 / 0.0030	5.23 / 0.0031	4.30 / 0.00215	1.20/1.40	1.21/1.44
4	Optical glass with LiNbO <sub>3</sub> Prism: 1.16×4.92×7.62	32.25 / 0.000407	29.4 / 0.00039	22.8 / 0.00065	1.41/0.62	1.29/0.60
5	Alumina (Al <sub>2</sub> O <sub>3</sub> ) (bulk) Prism: 5.88×6.70×8.14	9.35 / 0.00003	9.36 / 0.00003	9.38 / 0.00007	0.99/0.43	0.99/0.43
6	Sapphire (single crystal) Prism: 5.26×8.08×10.20	8.54 / 0.000015	8.87 / 0.000015	10.32 / 0.000017	0.83/0.88	0.79/0.88
7	MgTiO <sub>3</sub> (bulk sample) Prism: 4.62×8.32×9.90	14.35 / 0.000675	14.10 / 0.00064	17.90 / 0.005	0.80/0.14	0.91/0.13
8	Ferrite (16C44) Prism: 2.54×4.06×10.20	12.6 / 0.0018	13.2 / 0.0015	10.5 / 0.0026	1.20/0.69	1.25/0.58
9	Mica (multi-layer silicate) Prism: 2.720.80×8.50×10.34	4.87 / 0.00047	4.70 / 0.00050	3.0 / 0.0042	1.62/0.11	1.56/0.12
10	Crystalline Si for wafer Prism: 2.72×4.10×8.0	10.75 / 0.45	10.15 / 0.52	8.125 / 0.38	1.32/1.18	1.25/1.37
11	SI (semi-isolated) GaAs wafer Prism: 0.62×4.20×9.62	11.30 / 0.015	11.10 / 0.016	7.9 / 0.085	1.43/0.18	1.41/0.19

**Table 7.** Dielectric parameters and uni-axial anisotropy of disk carbon-content samples by single resonator method with different sample orientations (disk axis is orientated along Oz)

No	Material	$D, \text{ mm}; h, \mu\text{m}$	parallel: $\epsilon_{par}; \tan\delta_{\epsilon_{par}}$	perpendicular: $\epsilon_{perp}; \tan\delta_{\epsilon_{perp}}$	anisotropy: $A_{\epsilon}; A_{\tan\delta_{\epsilon}}$
1	Graphite (spectral pure)	$\phi$ 8.04; 3.18	135 (?) / 0.07 5.60 / 0.10 *)	15.9 / 0.0175	0.35/5.51
2	Air-filled Graphite	$\phi$ 6.74; 1.66	1.53 / 0.0192	1.65 / 0.0205	0.93/0.94
3	Graphene (pressed thick sample)	$\phi$ 5.92; 4.96	75 (?) / 0.25 4.08 / 0.15 *)	7.50 / 0.111	0.54/1.35
4	N-Graphene (pressed thick sample)	$\phi$ 8.74; 8.46	155 (?) / 0.4 4.25 / 0.27 *)	4.95 / 0.21	0.86/1.29

\*) measured by R1 resonator with TE<sub>011</sub> mode

and N-doped Graphene (the last two samples have been submitted from IST, Lisbon). The air-filled Graphite acts as isotropic foam-like material with big losses. The perpendicular permittivity of other materials has been measured without any problems – the obtained values are ~4.95 for N-Graphene, ~7.50 for pure Graphene and up to 15.9 for pure Graphite. However, in the case of the parallel orientation of the sample the resonance frequencies for all samples decrease considerably, for which the simulator gives very high permittivity values – up

to 75–155, which is quite unrealistic for the considered samples. In fact, we found out the reasons. In the simulations for the considered resonance structure: R2 resonator with disk sample placed vertically (as in Fig. 2c, Pos. 3), we can replace the sample with an ideal metal disk; Now the calculated resonance frequency is close to the measured ones. This fact shows that the screening effect of the resonator walls and in the considered high-conductivity carbon samples cannot give possibility of the E fields to penetrate deeply in the sample in this

**Table 8.** Dielectric parameters and uni-axial anisotropy of cylinder resonator with different composition and temperature conditions for material sintering

No	Material	$D, h, \text{mm}$	parallel: $\epsilon_{par}; \tan\delta_{epar}$	perpendicular: $\epsilon_{perp}; \tan\delta_{eperp}$	anisotropy: $A_e; A_{\tan\delta_e}$
1250 °C					
1	$\text{Ba}_{1.95}(\text{Li}_{0.5}\text{La}_{0.5})_{0.05}\text{Ti}_9\text{O}_{20}$	$\phi$ 9.10; 5.06	29.10/0.00019	22.30/0.00020	1.30/0.95
2	$\text{Ba}_{1.90}(\text{Li}_{0.5}\text{La}_{0.5})_{0.05}\text{Ti}_9\text{O}_{20}$	$\phi$ 9.10; 5.14	31.50/0.00034	22.00/0.00030	1.43/1.12
3	$\text{Ba}_{1.85}(\text{Li}_{0.5}\text{La}_{0.5})_{0.05}\text{Ti}_9\text{O}_{20}$	$\phi$ 9.10; 5.00	30.80/0.00049	22.80/0.00043	1.35/1.13
4	$\text{Ba}_{1.80}(\text{Li}_{0.5}\text{La}_{0.5})_{0.05}\text{Ti}_9\text{O}_{20}$	$\phi$ 9.00; 5.10	35.50/0.00079	28.60/0.00069	1.24/1.14
1300 °C					
5	$\text{Ba}_{1.95}(\text{Li}_{0.5}\text{La}_{0.5})_{0.05}\text{Ti}_9\text{O}_{20}$	$\phi$ 9.02; 4.88	29.98/0.00031	26.90/0.00029	1.11/1.07
6	$\text{Ba}_{1.90}(\text{Li}_{0.5}\text{La}_{0.5})_{0.05}\text{Ti}_9\text{O}_{20}$	$\phi$ 9.00; 4.88	32.55/0.00031	29.95/0.00018	1.09/1.74
7	$\text{Ba}_{1.85}(\text{Li}_{0.5}\text{La}_{0.5})_{0.05}\text{Ti}_9\text{O}_{20}$	$\phi$ 9.00; 4.68	33.55/0.00048	36.10/0.00037	0.93/1.32
7	$\text{Ba}_{1.80}(\text{Li}_{0.5}\text{La}_{0.5})_{0.05}\text{Ti}_9\text{O}_{20}$	$\phi$ 9.00; 4.90	34.60/0.00050	37.05/0.00040	0.93/1.32
1350 °C					
9	$\text{Ba}_{1.95}(\text{Li}_{0.5}\text{La}_{0.5})_{0.05}\text{Ti}_9\text{O}_{20}$	$\phi$ 9.00; 4.88	30.23/0.00024	30.40/0.00019	0.99/1.26
10	$\text{Ba}_{1.90}(\text{Li}_{0.5}\text{La}_{0.5})_{0.05}\text{Ti}_9\text{O}_{20}$	$\phi$ 9.00; 4.76	33.70/0.00027	33.50/0.00020	1.01/1.35
11	$\text{Ba}_{1.85}(\text{Li}_{0.5}\text{La}_{0.5})_{0.05}\text{Ti}_9\text{O}_{20}$	$\phi$ 9.14; 4.74	31.20/0.00026	32.10/0.00022	0.97/1.19
12	$\text{Ba}_{1.80}(\text{Li}_{0.5}\text{La}_{0.5})_{0.05}\text{Ti}_9\text{O}_{20}$	$\phi$ 9.04; 4.90	32.85/0.00063	33.90/0.00061	0.97/1.03

geometry and the structure acts as a metal disk in  $\text{TM}_{010}$  mode resonator. Now the whole structure has behaviour as a re-entrant resonator with metal post in the middle – the resonance frequency decreases due to this metal post. That’s why, we tried another resonance configuration – resonator R1 with  $\text{TE}_{011}$  mode, where the screening effect is proven as small. Now we measure considerable more realistic values of the parallel permittivity –  $\sim 4.45$  for N-Graphene, 4.08 for pure Graphene and 5.6 for pure Graphite. These values are very close to the values, obtained by a transmission-line method, based on covered coplanar waveguides [16]. These investigations will continue in future.

The last example is connected with characterization of a set of ceramic cylindrical dielectric resonators with different composition and technology conditions. The investigated system is  $\text{Ba}_x(\text{Li}_{0.5}\text{La}_{0.5})_{0.05}\text{Ti}_9\text{O}_{20}$ , obtained by peroxomethod, where  $x$  is 1.95, 1.90, 1.85 and 1.80. The temperature conditions for the ceramics calcination are: 1250, 1300 and 1350 °C (these samples have been given up from the University of Chemical Technology and Metallurgy, Sofia). The results for the measured dielectric constant and dielectric loss tangent in parallel and perpendicular to the cylinder sample axis, as well as for the calculated anisotropy have been presented in Table 8.

The results show that the measured permittivity varies in the interval 22–37, while the dielectric loss tangent – in the interval 0.00018–0.00079.

Therefore, the conclusion is that the composition and the temperature conditions influence the dielectric properties of the considered material in a big degree. However, more interesting from the point of view of this paper is the behaviour of the anisotropy. At low ceramics calcination temperature 1250 °C the anisotropy is relatively big, however with the increasing of the temperature (1300 °C; 1350 °C) the anisotropy becomes smaller and even we can detect practical isotropy of the produced ceramic samples. This is a new very important circumstance from the application point of view.

## CONCLUSIONS

The main conclusion from the investigations in this paper is that the accurate characterization of the dielectric anisotropy of wide class of crystalline and crystalline-like materials is fully possible by the authorship two-resonator method and its variants. The determination of the dielectric anisotropy (different permittivity and dielectric loss tangent in different directions) gives completely new additional information for the crystalline sample properties, richer than the simple determination of the permittivity and dielectric loss tangent. The origin of the dielectric anisotropy for crystalline samples is mainly connected with existence of predominant orientation of the building blocks (grains) of the structure due to specific reasons – crystallization, reinforce-



ing, vacuum evaporation of orientated inclusions, pressing, layering, sintering, etc. Therefore, the anisotropy is very informative parameter for clarifying the specificity of the used technological process and the samples composition. The obtained results show also that anisotropy is bigger for single-crystalline samples in comparison to the poly-crystalline samples from the same material. The sample homogenization is possible for some technological processes, e.g. fusing. The sintering at high temperature also can decrease the anisotropy. The results for the anisotropy of some carbon-content samples: Graphene and Graphite, are presented for the first time.

**Acknowledgements:** *The investigations have been supported financially by the National Research Fund in Bulgaria under Contract DN07-15. The authors would like to thank to different their colleagues from Faculty of Physics of Sofia University and University of Chemical Technology and Metallurgy, Bulgaria, Technical University, Sofia for the given samples.*

#### REFERENCES

1. P. R. Andrade, and S. P. S. Porto, *Annu. Rev. Mater. Sci.*, **4**, 287 (1974) <https://doi.org/10.1146/annurev.ms.04.080174.001443>
2. L. F. Chen, C. K. Ong, C. P. Neo, V. V. Varadan, V. K. Varadan, *Microwave Electronics: Measurement and Materials Characterization*, John Wiley & Sons Ltd., England, 2004 (Ch. 5/8).
3. P. I. Dankov, *IEEE Trans. MTT*, **54**, 1534 (2006)
4. V. N. Levcheva, B. N. Hadjistamov, P. I. Dankov, *Bulg. J. Phys.*, **35**, 33 (2008)
5. P. I. Dankov, in: *Microwave and Millimeter Wave Technologies from Photonic Bandgap Devices to Antenna and Applications*, Igor Minin (ed.), In-Tech Publ., Austria, 2010, ISBN 978-953-7619-66-4.
6. P. I. Dankov, B. N. Hadjistamov, I. I. Arestova, V. P. Levcheva, *PIERS Online*, **5**, 6, 501 (2009).
7. ANSYS HFSS, <https://www.ansys.com/products/electronics/ansys-hfss>
8. K. S. Cole, R. H. Cole, *J. Chem. Phys.*, **9**, 341 (1941)
9. A. Badev, I. Iliev, J. P. Cambronne, T. Lebey, A. Barnabe, V. Levcheva, *Optoelectron. Adv. Mater. – Rapid Commun.*, **1**, 10, 207 (2007).
10. P. I. Dankov, V. P. Levcheva, I. I. Arestova, in: *Proc. ICMF'2007*, Budapest, Hungary, 2007, p. 27.
11. P. Dankov, S. Kolev and S. Ivanov, in: *Proc. 17<sup>th</sup> EM Field & Materials*, Warsaw, Poland, 2004, p. 89.
12. V. P. Levcheva, I. I. Arestova, B. R. Nikolov, P. I. Dankov, *Telfor. J.*, **1**, 2, 57 (2009).
13. P. I. Dankov, M. I. Tsatsova, V. P. Levcheva, in: *Proc. of PIERS 2017*, Singapore, 2017 (online available on IEEE Xplore).
14. P. I. Dankov, in: *Proc. 47th EuMC2017*, Nuremburg, Germany, 2017, p. 954.
15. P. I. Dankov, in: *Proc. 48th EuMC2018*, Madrid, Spain, 2018, p. 335.
16. P. Dankov, invited paper in: *8th International Workshop and Summer School on Plasma Physics (IWSSPP'2018)*, Kiten, Bulgaria, 2018 (to be published in IOP Conference Series 2019).
17. U. Fritsch, I. Wolff, in: *Proc. IEEE MTT-S Digest*, 1992, p. 1131.
18. R. P. Owens, J. E. Aitken, T. C. Edwards, *IEEE Trans. MTT*, **8**, 499 (1976).
19. S. A. Ivanov, P. I. Dankov, *J. Electrical Engineering (Slovakia)*, **53**, 9s, 93 (2002).
20. G. Mumcu, K. Sertel, J. L. Volakis, *IEEE Trans. MTT*, **56**, 217 (2008).